On the Feasibility of CFD for Transient Airflow Simulations in Buildings

Nina Morozova, Roser Capdevila, F.Xavier Trias and Assensi Oliva
Heat and Mass Transfer Technological Center (CTTC), Universitat Politècnica de Catalunya - BarcelonaTech (UPC), ESEIAAT, C/ Colom 11, 08222, Terrassa (Barcelona), Spain
Corresponding author: nina@cttc.upc.edu

Abstract

The rapidly growing computational capacity has made CFD simulations an attractive tool for indoor environmental applications. The ability of CFD to perform transient simulations could be incorporated into model predictive control systems for buildings in order to correctly reproduce prompt disturbances in the air field, such as opening doors and windows or changes in occupants behaviour. In this work, two characteristic configurations which mimic typical airflow patterns inside buildings are studied using different grid sizes and turbulence models. Case one is a tall turbulent differentially heated cavity and case two is the turbulent mixed convection in a ventilated square cavity. The Spearman's rank correlation coefficient for transient simulations is compared against computational time for different CFD approaches, and the possibility of performing real-time simulations is evaluated. Among different turbulence models studied, the no-model approach with symmetry preserving discretization has shown the best overall performance in terms of computational cost and accuracy of the results.

Introduction

The proper function of heating, ventilation and air conditioning (HVAC) systems has a direct impact on occupants thermal comfort, which has a big influence on their productivity and satisfaction. Nowadays the majority of HVAC systems are mechanical and account for approximately 76% of the overall energy consumption in the residential and commercial buildings, according to IEA (2008). The rapidly increasing demand for energy efficiency and the long lifespan of the buildings makes fast calculation of indoor air distribution important for a vast number of applications, including the design of efficient ventilation setups and model predictive control (MPC) of building HVAC systems using real-time weather and occupants behaviour data.

The air distribution in the buildings can be evaluated by analytical or empirical models, as well as computer simulations. The latter allows a high degree of flexibility in addressing the problems, while analytical and empirical models do not permit to describe indoor airflow in its full complexity. The main tools for computer simulations of indoor environments are the multizone (airflow network) models, zonal models and Computational Fluid Dynamics (CFD) (Chen (2009). Multizone models have both the lowest computational cost and the lowest accuracy, while CFD simulations provide detailed and accurate information about indoor air flow at the expense of higher computational effort.

One of the remaining challenges in CFD for building simulations is inexpensive turbulence modelling (Li and Nielsen (2011). Three main approaches to model transient turbulent flow are Direct Numerical Simulation (DNS), Large Eddy Simulation (LES) and Unsteady Reynolds Average Navier-Stokes (URANS). DNS directly resolves all the turbulent flow scales, which makes it the most accurate and the most computationally expensive method. LES models resolve only big scales of motion and model the small ones, while URANS separates the time scales of the mean flow and models its turbulent fluctuations. LES models are normally more computationally expensive than URANS, but both methods have a reduced computational cost compared to DNS.

Wang and Zhai (2012) have investigated the credibility of coarse-grid CFD simulations and optimized the spacial discretization in order to reduce the total truncation error. In another study, Wang et al. (2014) have proposed to use numerical viscosity to model the effect of turbulence for coarse-grid CFD which helped to achieve a significant reduction in the computing speed. Capabilities of CFD to simulate indoor airflow have also been studied by Kempe and Hantsch (2017). They performed LES simulations of a model room with a heat source and concluded that real-time LES simulations can be carried out with high accuracy at moderate numerical effort. However, the possible industrial applications of real-time CFD simulations for HVAC systems have not been discussed in details.

Traditionally, CFD simulations of indoor environment are focused on steady calculations, because the building dynamics are slow. But at the same time the airflow inside the building is subject to intermittent disturbances caused by opening doors and windows,

occupants behaviour, weather changes, etc. The importance of correct caption of such a disturbances is shown by Choi and Edwards (2011), they have investigated the effect of human and door motions of the contaminant transport using transient CFD simulations. For the purpose of building design all these disturbances could be neglected, but they play a major role in model predictive control applications. Typically MPC systems have a control horizon range of 4-5 h, with a time step of 1-3 h (Afram and Janabi-Sharifi (2014)) which is a relatively short time period in building dynamics scale. In order to develop good quality models, transient simulations should be carried out, which would help to accurately capture the process dynamics.

The scope of this paper is to investigate the capabilities of CFD to perform transient simulations of indoor environment with relatively low computational cost and adequate accuracy in order to be used in MPC. Two representative cases were considered, namely a tall differentially-heated cavity and a ventilated cavity with heated floor. Both cases were tested on a wide range of computational grid resolutions together with different LES and RANS turbulence models. Finally, the possibilities of using transient CFD for short term thermal behavior prediction in building are discussed.

Physical problems and governing equations

Governing equations

The incompressible Navier-Stokes equations for Newtonian fluid with constant physical properties are considered. The Boussinesq approximation is adopted to account for the density variations due to temperature difference. Thermal radiation is neglected. Under these assumptions, the governing equations are

$$\nabla \cdot \mathbf{u} = 0 \tag{1}$$

$$\frac{\partial \mathbf{u}}{\partial t} + (\mathbf{u} \cdot \nabla)\mathbf{u} = \nu \nabla^2 \mathbf{u} - \frac{1}{\rho}\nabla p + \beta g (T - T_0) \tag{2}$$

$$\frac{\partial T}{\partial t} + (\mathbf{u} \cdot \nabla) T = \alpha \nabla^2 T, \tag{3}$$

where $\mathbf{u}$ is the velocity vector, t the time, p the pressure, T the temperature, T_0 the reference temperature, ν the kinematic viscosity, ρ the density, g the gravitational acceleration, β the thermal expansion coefficient and α the thermal diffusivity. Hereafter, all the results are presented in the dimensionless form. The reference values of time, velocity, temperature and length are specified for each problem separately.

Differentially heated cavity

Air flow inside a tall cavity. driven by the buoyancy forces is considered in this work. The objective of this flow configuration is to mimic a highly stratified turbulent indoor environment driven by the natural convection. This flow pattern could be found, for example, in tall building atria with one wall exposed to solar radiation. Moreover this configuration could be used as a simplified model of a complete building. This flow configuration is difficult to resolve correctly using other building modelling tools.

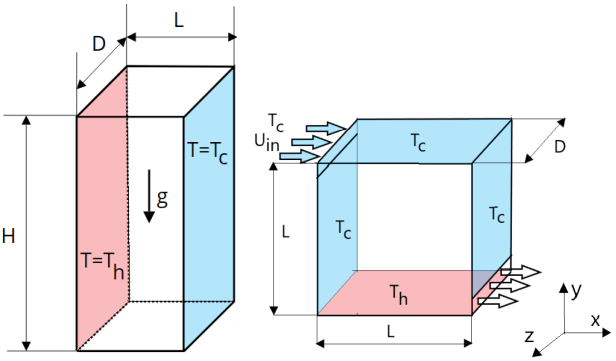

Figure 1: Geometry definition of the differentially heated cavity case (left) and the mixed convection in a ventilated cavity case (right).

The cavity has a height aspect ratio of $A_h = H/L = 3.84$ and a depth aspect ratio of $A_d = D/L = 0.86$ (Figure 1). The Prandtl number corresponds to air and is equal to $Pr = \nu/\alpha = 0.71$, where α is the thermal diffusivity and the Rayleigh number (based on the cavity height) is $Ra = g\beta\Delta T H^3/(\nu\alpha) = 1.2 \times 10^{11}$, where ΔT is the temperature difference, $T_h - T_c$. This configuration resembles the experimental set-up performed by Saury et al. (2011).

Two opposite vertical walls of the cavity in the x direction are maintained at uniform but different temperatures $T_h = 0.5$ at $x = 0$ and $T_c = -0.5$ at $x = L$. The temperature at the rest of the walls is given by the "Fully Realistic" boundary conditions proposed by Sergent et al. (2013), which are time independent analytical functions based on the experimental data. No-slip boundary condition is imposed on the walls. Zero values for all the variables are imposed for this test case as an initial condition.

For this test case the reference length is H and the reference time, velocity and temperature used for the dimensionless form are, respectively, $Ra^{1/2}H^2\alpha^{-1}, Ra^{1/2}(\alpha/H), \Delta T$.

Table 1: Computational grids used for the simulations of the differentially heated cavity case.

Case	N_x	N_y	N_z	N_{total}
M1	8	30	4	9.60×10^2
M2	10	40	6	2.40×10^3
M3	12	50	8	4.80×10^3
M4	14	60	10	8.30×10^3
M5	18	80	12	1.73×10^4
M6	24	100	16	3.84×10^4
M7	30	120	20	7.20×10^4
M8	40	150	24	1.44×10^5
M9	50	180	30	2.70×10^5
M10	70	240	40	6.72×10^5
M11	100	320	40	1.28×10^6
REF	140	500	70	4.90×10^6

Eleven different structured grids have been used in the numerical tests and are detailed in Table 1. All the grids are Cartesian, uniform in the vertical (y) and spanwise (z) directions and refined near the walls using a hyperbolic tangent function in the horizontal (x) direction with the concentration factor $\gamma_x = 2$.

Mixed convection in a ventilated cavity

The second test case considered in this paper is a 3D ventilated cavity with heated floor. This configuration was first studied experimentally by Blay et al. (1992) and later numerically by Ezzouhri et al. (2009). The geometry of the studied cavity is shown in the Figure 1. The height aspect ratio of the cavity is $A_h = L/L = 1$ and the depth aspect ratio is $A_d = D/L = 0.3$. The cold air with parameters $T_c = -0.5, U_{in} = 1$ enters through the long thin inlet slot with an aspect ratio $A_{in} = L_{in}/L = 0.017$ at the top of the left wall of the cavity and is discharged through the outlet slot with and aspect ratio $A_{out} = L_{out}/L = 0.023$ at the bottom of the right wall of the cavity. Bottom wall is maintained at the hot temperature $T_h = 0.5$, while three other side walls are kept at the cold temperature $T_c = -0.5$. Front and rear walls are adiabatic.

The cavity is filled with air with $Pr = 0.71$, Rayleigh number based on the cavity height is equal to $Ra = 2.4 \times 10^9$ and the Froude number based on the inlet height is equal to $Fr = U_{in}/\sqrt{g\beta\Delta T L_{in}} = 5.24$. The inlet velocity profile is parabolic in vertical y direction with respect to the measured velocity profile and uniform in the normal z direction. At the outlet, convective boundary conditions are imposed for the velocity and pressure and zero-gradient is imposed for the temperature. No-slip boundary condition is applied on the solid walls. The initial conditions for this case are: $\mathbf{u}_{ini} = 0, p_{ini} = 0$ and $T_{ini} = T_c$.

In this test case, the reference values used for non-dimensionalizing are the length L, the time U_{in}/L, the velocity U_{in} and the temperature $(T - T_{mean})/\Delta T$, where T_{mean} is the mean temperature equal to $(T_h + T_c)/2$.

This configuration is very important for indoor environmental applications. Apart from representing the typical ventilated room with thermal exhausts coming from its lower part, it is also a vivid example of the flow solution multiplicity. At the certain inlet velocity the main air vortex could move clockwise or counterclockwise as was observed in Ezzouhri et al. (2009). This phenomenon cannot be correctly reproduced by either zonal or multizone models, while correct solution of the flow is crucial for the correct design of the HVAC systems.

Eleven different structured grids detailed in Table 2 have been used for this test case. All grids are uniform in the spanwise (z) direction and zones of inlet (N_{in}) and outlet (N_{out}) only in vertical (y) direction. In the horizontal (x) direction and the main zone of the vertical (y) direction grids are refined near the walls using a hyperbolic tangent function with the concentration factors $\gamma_x = 1.5$ and $\gamma_y = 2$.

Simulations for both cases are carried out for 25 non-dimensional time units. which was found to be long enough for capturing the transient flow dynamics.

Table 2: Computational grids used for the simulations of the mixed convection case.

Case	N_x	N_y	N_z	N_{in}	N_{out}	N_{total}
M1	10	10	4	2	3	6.00×10^2
M2	15	20	4	2	3	1.20×10^3
M3	20	25	4	2	3	2.40×10^3
M4	25	25	6	3	4	4.80×10^3
M5	30	25	10	3	4	9.60×10^3
M6	40	32	12	3	5	1.92×10^4
M7	45	40	16	4	6	3.60×10^4
M8	60	48	20	4	8	7.20×10^4
M9	75	64	24	6	10	1.44×10^5
M10	96	80	30	8	12	2.88×10^5
M11	120	94	40	10	16	5.76×10^5
REF	150	120	50	20	20	1.20×10^6

Numerical methods

Two different software have been used to perform the simulations: OpenFOAM (Weller et al. (1998)) for unsteady RANS approach and TermoFluids software (TermoFluids S.L. (2019)) for LES turbulence models. Both software use finite-volume discretization on collocated grids.

Reynolds-averaged Navier-Stokes approach

The RANS approach is based on time-averaged filtering of the governing equations 1- 3. It calculates statistically-averaged (Reynolds-averaged) variables and approximates the turbulence fluctuation effect on the mean flow using different turbulence models.

Unsteady RANS (URANS) models are developed by separating the time scales of the mean flow and the turbulent fluctuations. In this work URANS simulations are performed using the OpenFOAM (Weller et al. (1998)) software using transient *"buoyantBoussinesqPimpleFoam"* solver for buoyant, turbulent flow of incompressible fluids to solve pressure-velocity linkage in means of Boussinesq approximation and PIMPLE algorithm.

RANS eddy-viscosity models are based on the resolution of turbulent viscosity by means of two different turbulent quantities: the turbulent kinetic energy (k) and another turbulent quantity related to its dissipation. In case of $k-\epsilon$ family of models it is dissipation rate of turbulent kinetic energy (ϵ), and for $k-\omega$ models it is turbulent kinetic energy dissipation (ω).

Based on the findings of Morozova et al. (2018) and Zhai et al. (2007), the $k-\epsilon$ turbulence model was chosen for transient simulations of indoor airflow. For steady calculations $k-\epsilon$ model has shown the smallest computational cost and the most accurate results

among all tested RANS models.

Large Eddy Simulation approach

A different approach for turbulence modelling is LES, where the large scale of turbulent motions are resolved, whereas the effects of the smallest-scale motions are modelled by means of a subgrid-scale (SGS) model. The spatial discretization in LES simulations is carried out using a symmetry preserving discretization on structured collocated Cartesian grids (Trias et al. (2014)). Pressure and velocity coupling is solved using a fractional step method. LES simulations are carried out using the in-house CFD code Termofluids.

A one-parameter fully explicit second-order one-leg temporal discretization scheme (Trias and Lehmkuhl (2011)) is used for time integration. Based on the recommendations by Morozova et al. (2018) and Zhai et al. (2007), LES-WALE SGS model and no-model approach are chosen for further tests.

In WALE subgrid scale model, the calculation of the eddy-viscosity is based on the square of the velocity gradient tensor, which takes into account the shear stress tensor as well as the rotation tensor. Both LES-WALE and no-model approaches have shown a good trade off between computational cost and accuracy comparing to other LES models.

Results and discussion

This section is dedicated to presentation of the simulation results, their convergence and the discussion on the feasibility of transient CFD simulations of the indoor environments. Results of CFD simulations with different turbulence models and grids sizes are presented and discussed.

The feasibility of CFD to perform transient or steady simulations of indoor environment is always a compromise between the computational cost and accuracy. HVAC applications normally have very limited computational resources available. Moreover, simulations normally need to be carried out for each building individually. Despite the high computational cost, CFD could offer many advantages which other building simulation tools do not possess. The ability to perform transient simulations is one of the most interesting advantages.

In building simulations, the overall accuracy of the simulations is more important than correct prediction of the airflow parameters in an specific location. In order to evaluate the overall accuracy of the simulations, four global quantities have been chosen for comparison: average kinetic energy (Eq. 4), average enstrophy (Eq. 5), average Nusselt number at the hot wall (Eq. 6) and the average temperature at the center of the cavity. Average Nusselt number and temperature represent the thermal properties of the flow, average kinetic energy is used to quantify the overall level of motion and average enstrophy corresponds to dissipation effects in the fluid. The global quantities are defined as follows:

$$E = \int_V \frac{\mathbf{u}^2}{2} dV \tag{4}$$

$$\Omega = \int_V \boldsymbol{\omega}^2 dV \tag{5}$$

$$Nu = \int_0^H \frac{\partial T}{\partial x} dy \bigg|_{x=0}, \tag{6}$$

where V is the volume of the cavity and $\boldsymbol{\omega} = \nabla \times \mathbf{u}$ is the vorticity.

The quality of transient simulations is investigated using Spearman's rank correlation coefficient r_s, which is a measure of rank correlation. Spearman's rank correlation shows monotonic nonlinear relationships between two functions, the values of the coefficient fluctuate between 1 (perfectly correlated values) and -1 (perfectly uncorrelated values) and are calculated using equation 7:

$$r_s = \frac{\Sigma_i (a_i - < a >)(b_i - < b >)}{\sqrt{\Sigma_i (a_i - < a >)^2 \Sigma_i (b_i - < b >)^2}}, \tag{7}$$

where a_i, b_i are the i-th members of the compared sets of data and $< a >, < b >$ are the mean values of the same sets of data.

All simulations are preformed using AMD Opteron 2350 processor machine with $24Gb/s$ memory bandwidth. The number of CPU cores, used for the parallel simulations varies between 1 and 32. This was done in order to speed up the computational process. But later the simulation time was rescaled to Intel Core i7-8700K processor with 6 CPU cores and $41.6Gb/s$ memory bandwidth. Since this processor is widely used in modern workstations. However simulations could be performed either on conventional office workstation or on the cloud platforms.

The behaviour of the solvers has been assumed to be ideal, so simulations are rescaled using linear dependencies of processors memory bandwidth, number of CPUs and number of nodes. Rescaled target time, t_{tgt} is calculated as follows:

$$t_{tgt} = t_{ref} \frac{BW_{ref}}{BW_{tgt}} \frac{CPU_{ref}}{CPU_{tgt}} \frac{NODE_{ref}}{NODE_{tgt}}, \tag{8}$$

where t_{ref}, t_{tgt} are the reference and target computational time, BW_{ref}, BW_{tgt} the reference and target processor bandwidth, CPU_{ref}, CPU_{tgt} the reference and target number of CPUs and $NODE_{ref}, NODE_{tgt}$ are the reference and target number of nodes respectively.

The indicator to evaluate the performance of the solvers is the time ratio $R = t_{wc}/t_{phy}$ between the wall-clock time for the computation, t_{wc}, and physically simulated time, t_{phy}. A simulation is faster than real-time when $R < 1$.

In the field of model predictive control for buildings, the simulation time plays a crucial role in the con-

troller performance. The control horizon range normally varies between 4 to 5 hours. This value refers to the length of the time for which the control signal is computed. A typical time step for MPC systems is around 1 to 3 hours (Afram and Janabi-Sharifi (2014)). Therefore, it could be inferred that the CFD simulations for MPC should be at least 5 times faster than real-time ($R \leq 0.2$), in order to be able to predict the airflow parameters 5 hours ahead of the time with 1 hour time step (the worst case scenario).

In the next two subsections results of the two aforementioned test cases are discussed in details using the methodology presented above.

Differentially heated cavity

For the differentially heated cavity case three global quantities were considered: average Nusselt number on the hot wall (Eq. 6), average kinetic energy (Eq. 4) and average enstrophy (Eq. 5). Simulation results are compared to the LES results on a fine grid (REF mesh in Table 1) due to the lack of transient experimental or DNS results. Time evolution of these quantities is shown in Figures 2-4 (top). The time evolution is plotted for mesh M4 with no-model approach, M5 for LES-WALE and M1, M11 for URANS $k-\epsilon$. In Figures 2-4 (bottom) the Spearman's correlation coefficients of these quantities are plotted against the computational time ratio R in logarithmic scale. Each point of the graph represents a mesh from Table 1. Thick horizontal dash line separate the area within 15% error from the value of perfect correlation ($r_s = 1$).

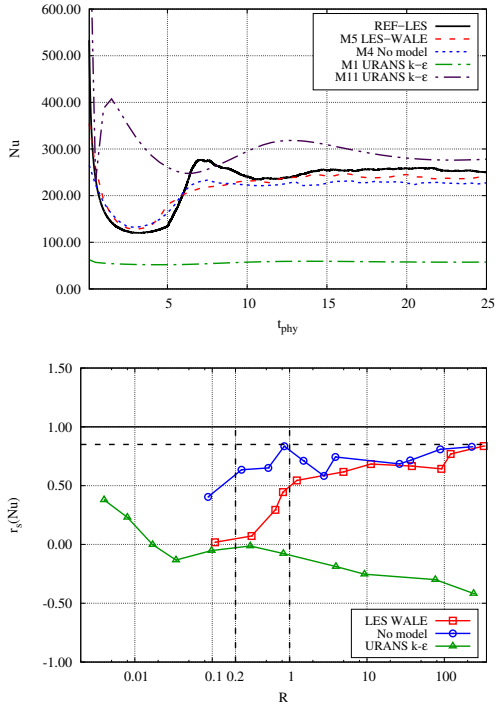

Figure 2: The time evolution of the average Nusselt number on the hot wall (top) and its Spearman's rank correlation coefficient for different grids and turbulence models against the time ratio R (bottom) for the differentially heated cavity case.

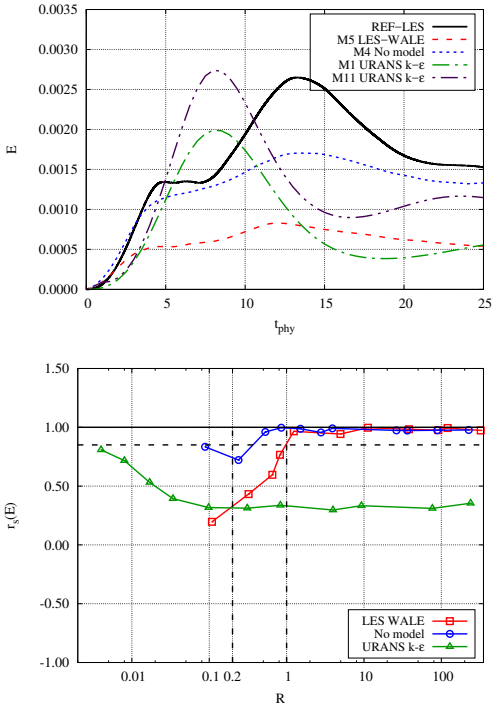

Figure 3: The same caption as Figure 2, but for the kinetic energy and differentially heated cavity case.

Nusselt number (Figure 2) is the fastest quantity to converge to steady state. The development of the quantity starts with the drop to the minimum value at the time $t_{phy} \approx 3$ then at the time $t_{phy} \approx 6$ the maximum peak is observed. LES and no-model cases behave similar to the reference solution and tend to converge towards perfect correlation. However, URANS model shows negative correlation due to the fact its transient behaviour is completely different from that of LES. The no-model approach shows the best correlation for Nu, meanwhile URANS $k-\epsilon$ model gives correlation with negative tendency.

Kinetic energy (Figure 3) is reaching its maximum at time $t_{phy} \approx 14$ for LES and no-model cases, while for the URANS simulations the maximum appears earlier at $t_{phy} \approx 8$. Then, all the approaches are smoothly converging to the statistically-steady values. LES and no-model approach show very good correlation tendency at the mesh resolution M5 and M4, respectively, and on finer grids. On the other hand, URANS again exhibits negative correlation because of the early peak.

Enstrophy (Figure 4) is showing a behaviour similar to the kinetic energy. Reference simulation has two peaks at $t_{phy} \approx 4$ and $t_{phy} \approx 12$ and a minimum at $t_{phy} \approx 9$. URANS results for mesh resolution M11 predict only the first peak, while the second peak is almost dissipated. LES and no-model approaches show very good transient correlation with the mesh resolution M5 and M4, respectively, and finer. However, URANS approach does not correlate well even thought it shows a positive tendency.

In overall for the differentially heated cavity test case, the no-model approach gives the best transient corre-

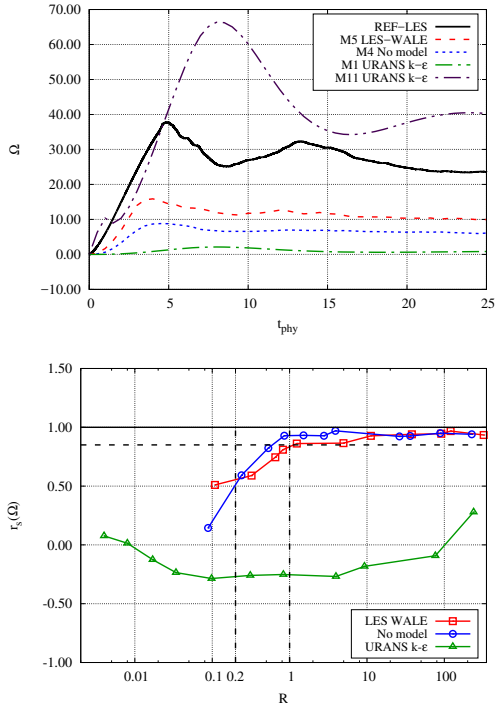

Figure 4: The same caption as Figure 2, but for the enstrophy and differentially heated cavity case.

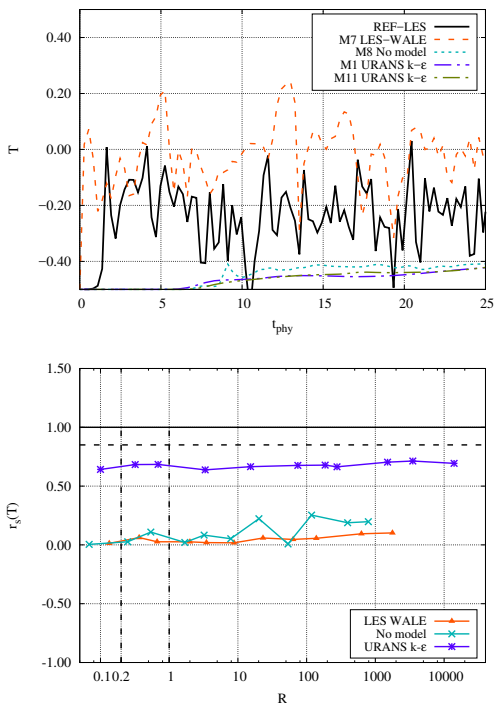

Figure 5: The same caption as Figure 2, but for the temperature at the center of the cavity and mixed convection case.

lation at the coarsest mesh resolution (M4) with time ratio $R \approx 1$ close to the real-time simulation.

Mixed convection

For this simulation three global quantities are considered: average kinetic energy (Eq. 4), average enstrophy (Eq. 5) and temperature at the center of the cavity. Time evolution of these quantities is presented in Figures 5-7 (top) and their associated Spearman's correlations are plotted against the time ratio R in Figures 5-7 (bottom). Again, LES results on a fine grid (REF mesh in Table 2) is used as reference.

Average temperature at the center of the cavity is a highly fluctuating quantity and it is difficult to predict its transient evolution (Figure 5). However, unlike LES, URANS and no-model approaches show smooth temperature profile that rapidly converges to a statistically steady state value. Two different patterns of transient behaviour explain the low values of correlation coefficients which almost do not depend on the mesh resolution.

Time evolution of kinetic energy for the mixed convection is easier to predict than temperature (Figure 6). The first peak value is reached at time $tt_{phy} \approx 10$ and the second peak appears at $t_{phy} \approx 20$. LES and no-model simulations repeat both peaks and show a good level of correlation. URANS approach also successfully predicts both peaks, but with a time shift of approximately 2 time units. For kinetic energy of the mixed convection test case all three tested approaches show a good transient correlation.

The behaviour of the time evolution of the enstrophy is predicted well by LES and no-model simulations (Figure 7), meanwhile the predictions of URANS are very different. URANS is converging smoothly, while other approaches show peaks at $t_{phy} \approx 12$ and $t_{phy} \approx 21$. This is illustrated by the low values of the correlation coefficient for URANS models.

Despite the fact that this test case is less turbulent than the previous one, it is more challenging to solve because of the hypothetical backwards flow at the outlet and two possible directions of the main vortex rotation. The complexity of the physics of the problem explains the obtained results. For this test case, LES approach gives the best transient correlation at the lowest mesh resolution (M7) with time ratio $R \approx 23$.

Potential of accessing transient CFD simulations for MPC applications

As mentioned, in order to incorporate CFD simulations into building energy control systems, they should be at least 5 times faster than real-time ($R \leq 0.2$). At the same time they should be performed using office workstation computers. The required simulation accuracy highly depends on the controlled building's function. Civil buildings like offices or residential buildings have a bigger range of acceptable air parameters than, for example, hospitals or server rooms. It could be assumed that 15% error in the prediction of the transient evolution of global quantities is sufficient for civil buildings applications.

With the current computational power it is not possible to incorporate CFD simulations into MPC system of a building. However, taking into account the law of growing processors capacity proposed by Moore (1965), the time in which transient CFD applications

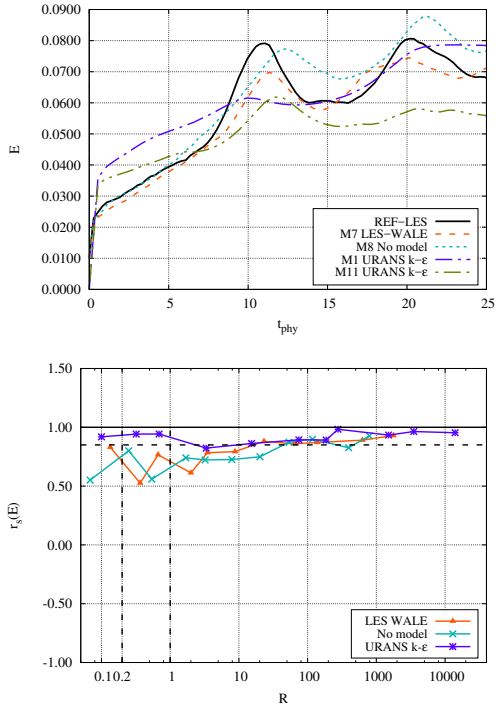

Figure 6: The same caption as Figure 2, but for the kinetic energy and mixed convection case.

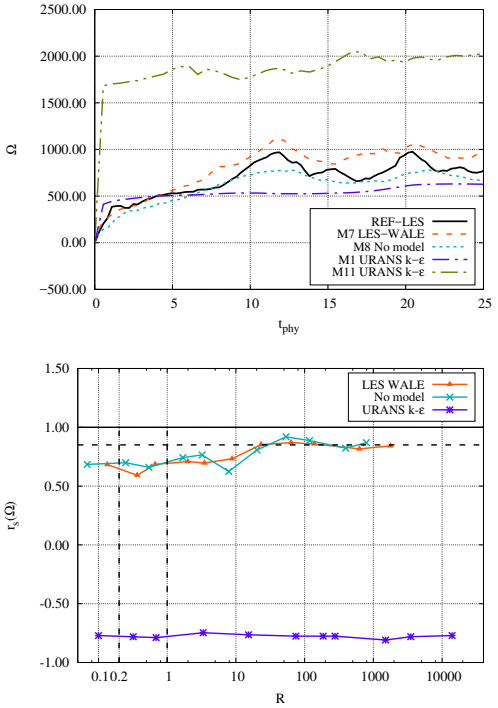

Figure 7: The same caption as Figure 2, but for the enstrophy and mixed convection case.

would be available for building control purposes could be estimated (Figure 8). The Moore's law states that the number of transistors in a dense integrated circuit would double in about every 18 months.

The required mesh resolution and the computational resources for different test cases vary significantly. For a closed system like the differentially heated cavity test case, good temporal correlation for the mesh with 8.30×10^3 control volumes with required time ratio ($R \leq 0.2$) could be achieved within the next 5 years. However, an open system like the mixed convection case needs a spatial resolution of at least 3.60×10^4 control volumes to perform correct transient simulations, which postpones the availability to withing the next 10 years.

Conclusions

Transient CFD simulation is a promising tool for MPC systems in buildings since it provides the user with a complete set of airflow parameters at every point of the building or room.

In this work two test cases have been studied using three different turbulence models in order to investigate the feasibility of transient CFD simulations for indoor environment. The Spearman's rank correlation coefficient is used to determine the quality of transient simulations and the time ratio is used for its computational cost evaluation. The no-model approach predicted global quantities transient correlation with less than 15% error with the time ratio $R \approx 1$ (mesh M4 in Table 1) for the differentially heated cavity case and with $R \approx 54$ (mesh M8 in Table 2) for the mixed convection case. LES-WALE model has shown time ratios of $R \approx 1.5$ (mesh M5

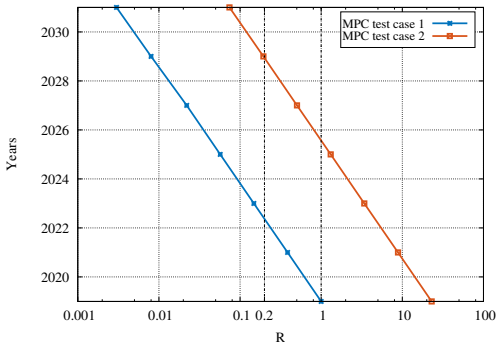

Figure 8: Potential availability of transient CFD simulations on office workstation computers for MPC systems over the next years.

in Table 1) and $R \approx 23$ (mesh M7 in Table 2) respectively. URANS $k - \epsilon$ model has not shown good transient correlation for any of the cases.

Turbulence modelling in coarse grid CFD simulations is not very beneficial. LES and no-model approaches have shown similar accuracy of the results, while the no-model approach has an approximately 10% lower computational cost. URANS has shown the lowest computational cost for the coarse grids, however, it increases exponentially for finer grids due to the large number of iterations of the pressure solver. Moreover, URANS approach failed to predict the transient evolution of the airflow correctly.

Nowadays it is not possible to use transient CFD simulations for MPC systems of the buildings. However, with the rapidly growing computational capacity, CFD would be feasible for control purposes on office workstations within the next 5 years for closed systems and withing 10 years for open systems.

The main direction of the future work is to opti-

mize the numerical algorithms of CFD simulations using GPU acceleration and to improve the numerical stability using a staggered symmetry-preserving discretization approach. The investigated test cases are of simplified geometry and do not take into account the effects of solar radiation, occupants behaviour, equipment heat emissions, etc., but for the future work more complicated cases will be considered. One more interesting idea for the future work is to develop a machine learning system of training CFD simulations on previously-run data sets. This could improve the predictions quality as well as reduce the computational cost.

Acknowledgments

This work has been financially supported by the Ministerio de Economía y Competitividad, Spain (No.ENE2017-88697-R). N.M. is supported by a FPU 2016 predoctoral contract (NoFPU16/06333) financed by Ministerio de Economía y Competitividad, Spain. F.X.T. is supported by a Ramón y Cajal postdoctoral Contract (No. RYC-2012-11996) financed by the Ministerio de Economía y Competitividad, Spain.

References

Afram, A. and F. Janabi-Sharifi (2014). Theory and applications of hvac control systems - a review of model predictive control (mpc). *Building and Environment 72*, 343–355.

Blay, D., S. Mergui, and J. T. amd F. Penot (1992). Experimental turbulent mixed convection created by confined buoyant wall jets. In *Proceedings of the First European Heat Transfer Conference*. UK.

Chen, Q. (2009). Ventilation performance prediction for buildings: A method overview and recent applications. *Building and Environment 44*(4), 848–858.

Choi, J. I. and J. R. Edwards (2011). Large-eddy simulation of human-induced contaminant transport in room compartments. *Indoor Air 22*(1), 77–87.

Ezzouhri, R., P. Joubert, F. Penot, and S. Mergui (2009). Large eddy simulation of turbulent mixed convection in a 3d ventilated cavity: Comparison with existing data. *International Journal of Thermal Sciences 48*(11), 2017–2024.

International Energy Agency (2008). *Energy Efficiency Requirements in Building Codes Energy Efficiency Policies for New Buildings*.

Kempe, T. and A. Hantsch (2017). Large-eddy simulation of indoor air flow using an efficient finite-volume method. *Building and Environment 115*, 291–305.

Li, Y. and P. V. Nielsen (2011). Cfd and ventilation research. *Indoor Air 21*(6), 442–453.

Moore, G. E. (1965). The future of integrated electronics. In *Fairchild Semiconductor internal manuscript*.

Morozova, N., R. Capdevila, F. Trias, and A. Oliva (2018, July 9-13,). Towards Real-Time CFD Simulation of Indoor Environment. In *Proceedings of 10th International Conference on Computational Fluid Dynamics*.

Saury, D., N. Rouger, F. Djanna, and F.Penot (2011). Natural convection in an air-filled cavity: Experimental results at large Rayleigh numbers. *International Communications in Heat and Mass Transfer 38*(6), 679–687.

Sergent, A., P. Joubert, S. Xin, and P. L. Quéré (2013). Resolving the stratification discrepancy of turbulent natural convection in deferentially heated air-filled cavities Part II: End walls effects using large eddy simulation. *International Journal of Heat and Fluid Flow 39*, 15–27.

TermoFluids S.L. (2006-2019). [http://www.termofluids.com/].

Trias, F. and O. Lehmkuhl (2011). A self-adaptive strategy for the time-integration of Navier-Stokes equations. *Numerical Heat Transfer, part B 60*(6), 116–134.

Trias, F., O. Lehmkuhl, A. Oliva, C. Pérez-Segarra, and R. Verstappen (2014). Symmetry-preserving discretization of Navier-Stokes equations on collocated unstructured grids. *Journal of Computational Physics 258*(1), 246–267.

Wang, H. and Z. Zhai (2012). Application of coarse-grid computational fluid dynamics on indoor environment modeling: Optimizing the trade-off between grid resolution and simulation accuracy. *HVAC&R Research 18*(5), 915–933.

Wang, H., Z. J. Zhai, and X. Liu (2014). Feasibility of utilizing numerical viscosity from coarse grid cfd for fast turbulence modeling of indoor environments. *Building Simulation 7*(2), 155–164.

Weller, H. G., G. Tabor, H. Jasak, and C. Fureby (1998). A tensorial approach to computational continuum mechanics using object-oriented techniques. *Computers in Physics 12*(6).

Zhai, Z., Z. Zhang, W. Zhang, and Q. Chen (2007). Evaluation of Various Turbulence Models is Predicting Airflow and Turbulence in Enclosed Environments by CFD: Part 2 - Comparison with Experimental Data from Literature. *HVAC&R Research 13*(6), 871–886.